Development of a calibration methodology to improve the on-site non-destructive evaluation of concrete durability indicators

Géraldine Villain, V. Garnier, Zoubir Medhi Sbartaï, Xavier Derobert, Jean-Paul Balayssac

Please cite the published version in Materials and Structures, 2018, https://doi.org/10.1617/s11527-018-1165-4

DEVELOPMENT OF A CALIBRATION METHODOLOGY TO IMPROVE THE ON-SITE NON-DESTRUCTIVE EVALUATION OF CONCRETE DURABILITY INDICATORS

G. Villain[1*], V. Garnier[3], Z. M. Sbartaï[4], X. Dérobert[1], J-P. Balayssac[2]

1 IFSTTAR, Nantes Site, Nantes, France
2 Université de Toulouse, UPS, INSA, LMDC, Toulouse, France
3 Université de la Méditerranée, LCND-LMA, Aix-en-Provence, France
4 Université de Bordeaux, I2M, Talence, France

***Corresponding author**, e-mail address: geraldine.villain@ifsttar.fr
Institut Français des Sciences et Technologies des Transports, de l'Aménagement et des Réseaux
IFSTTAR – Site de Nantes, MAST, LAMES, Allée des Ponts et Chaussées, CS4, F-44344 Bouguenais, France
phone: 33 (0)2 40 84 57 22, fax: 33 (0)2 40 84 59 97 (ORCID 0000-0002-4478-034X)

ACKNOWLEDGMENTS

The study presented herein is part of a French research project (C2D2-ACDC) conducted within the Urban and Civil Engineering Network (RGCU) and France's Ministry of Ecology, Sustainable Development and Energy (MEDDE). Thus, this research was funded by the RGCU Network and Ministry of Ecology, Sustainable Development and Energy. The authors would especially like to thank MEDDE's DRIEA Directorate. The authors are also grateful to both J. Salin (EDF) and V. Fardeau (CEREMA) for their valuable collaboration, as well as to O. Coffec and A. Joubert (IFSTTAR) for their high-level technical support.

ABSTRACT

This paper addresses the use of non-destructive testing (NDT) methods to assess indicators for both the concrete durability (porosity, degree of saturation) and mechanical properties (elasticity modulus, compressive strength) of reinforced concrete structures. NDT results, called "observables", are obtained by means of ultrasonic or electromagnetic methods and then correlated with these mechanical and durability indicators. The conversion model used to transform observables into indicators depends on the actual concrete mix design. If this conversion model is unavailable for the reinforced structure under study, then the evaluation may be inadequate due to

high uncertainty on the results. This paper proposes a calibration methodology to derive a conversion model appropriate for the structure by use of a minimum number of cores in order to improve the on-site evaluation. A motorway bridge is tested and characterized by NDT, after which some cores are extracted for calibration and others for validation. The cores are subsequently non-destructively characterized in the laboratory and/or used to determine indicators by means of standardized destructive methods. The non-destructive (ND) calibration protocol on cores is presented first. Next, NDT results recorded *in situ* and on the corresponding core are compared. Also, durability indicators deduced from on-site NDT measurements in addition to calibration are compared with reference durability indicators that have been independently determined by standard destructive methods. Results obtained by analyzing more than 1600 data fully validate the tested calibration methodology.

KEYWORDS

Porosity; water content; degree of saturation; resistivity; permittivity; GPR; ultrasonic velocity.

INTRODUCTION

In the field of civil engineering, non-destructive testing (NDT) is foreseen as a useful tool for engineers and facility owners to get quantitative indicators that allow establishing precise diagnoses and implementing maintenance programs for monitoring the structure conditions throughout its service life [1-4]. Performance-based approaches [5, 6] specify the most important durability indicators of concrete needed to be assessed, such as mechanical strength, porosity, water content or degree of saturation and transport coefficients.

Among these main indicators, porosity is an important factor, as it influences mechanical properties such as Young's modulus and strength, but also as it influences the durability of concrete. Indeed, porosity influences the transport coefficient (diffusion coefficient and permeability) and consequently the ingress of aggressive agents that cause reinforcement to corrode [5]. Porosity

conditions also the resistance to freeze-thaw cycles. Water content is another critical parameter, especially given that water is a common agent of most deterioration processes (e.g. corrosion, hydrate dissolution, freezing, alkali-aggregate reaction) and moreover controls the penetration kinetics of salt and carbon dioxide [5, 7, 8]. For this reason, porosity and degree of saturation (which is preferable to water content by virtue of being independent of porosity) are the most common parameters found in the durability models developed to predict the evolution of degradation and forecast the residual service life of reinforced concrete structures.

Some NDT techniques are sensitive to several concrete properties. For instance, ultrasonic (US) waves are mainly sensitive to porosity or mechanical properties, such as Young's modulus and compressive strength [9-12], yet are also affected by moisture variation [10-13]. Moreover, methods based on electromagnetic (EM) wave propagation [14-20], as well as electrical resistivity measurement methods [21-24, 17], are highly sensitive to water content and hence to the degree of saturation, while exhibiting less sensitivity to porosity [12, 25]. NDT techniques can be sensitive to the type of aggregate, cement or mineral additions, which explains why a calibration protocol has been developed to eliminate these constant biases. Due to the double dependency on porosity and degree of saturation, the cause of the measurement variation in the NDT parameter cannot be easily determined. Consequently, a combination of complementary methods is recommended in order to accurately assess the degree of saturation and porosity of concrete [12, 26-28]. When relying on such a combination procedure, it becomes possible to evaluate durability indicators and/or mechanical properties, as reported by several authors. The challenge however consists of transferring this methodology to real structures [29-31]. Though the NDT combination yields reliable results in laboratory measurements, only limited research has been dedicated to on-site applications. The NDT combination is not sufficient. Indeed, since laboratory concrete mixes differ from that of the investigated structure, the models identified from laboratory measurements are not directly applicable on-site in most cases [12]. In addition, other parameters can generate considerable noise (e.g. concrete surface quality, property gradients, skin and wall effects,

carbonation) [15, 32-34]. The need exists therefore for a methodology that adapts the laboratory procedure to a structure on site assessment. The general principle behind the proposed calibration methodology is based on a determination of models capable of converting ND observables to durability indicators on cores extracted from the studied structure. Thus, the conversion models (or calibration curves) obtained in this manner are more representative of the material properties of the surveyed structure.

In a context of built heritage preservation, it is very important to transfer the use of NDT from a laboratory setting to real structures for an optimal evaluation of the concrete durability indicator [31, 4]. The research presented seeks to assess concrete mechanical properties and durability indicators, both of which are key parameters in the physicochemical degradations and rebar corrosion of reinforced concrete structures. The mechanical and durability indicators studied are as follows: compressive strength Rc, secant Young's modulus E_{stat}, bulk porosity ϕ, and degree of saturation S. This paper focuses on the two indicators ϕ and S. The ultimate goal is to develop a methodology that allows obtaining calibration curves (i.e. a conversion model to transform the ND observables into ϕ and S) and then evaluating these durability indicators on a real structure by means of ND measurements.

The first part of this paper presents the three complementary NDT methods used to test cores (∅75x70 mm) in the laboratory. The second part is devoted to the calibration protocol, while Part 3 describes the on-site validation campaign, including ND testing and coring. The relevant test site is a highway bridge located in Marly (France). The final part is intended to compare laboratory and test site results, in addition to introducing literature results [35, 11, 12]. Estimated indicators are also compared with references in order to validate the protocol.

1 ND METHODS USED FOR IN-LABORATORY CALIBRATION

Three ND laboratory methods were designed to characterize same-sized cylindrical samples, with a diameter and height equal to 75 mm and 70 mm, respectively. These dimensions have been

set greater than 3 times the maximum diameter currently used for aggregates (20 mm) in order to generate a representative elementary volume of a heterogeneous material like concrete [1].

1.1 Ultrasonic waves in transmission

The ultrasonic (US) device, developed by Benmeddour *et al.* [36], serves to measure in transmission the velocity of compression (P) or shear (S) waves, whose central frequency equals 250 kHz. This device (see Fig. 1) is composed of: an amplifier-generator, 2 concentric transducers P and S, an amplifier for the transmitted signal, and an oscilloscope. For each sample, the mean signal (256 repetitions) is recorded 10 times in 10 different positions. The observables obtained are the P-wave velocity (*Vp*) and the S-wave velocity (*Vs)*. Knowing the sample density, the dynamic Young's modulus and Poisson's ratio can also be calculated. The *Vp* measured in the laboratory on a cylindrical sample can thus be compared to the P-wave velocity measured by transmission at the same on-site frequency [11] (see Section 3.2). The saturated concrete variation range of P-wave velocity is about 3500-5500 m/s [37].

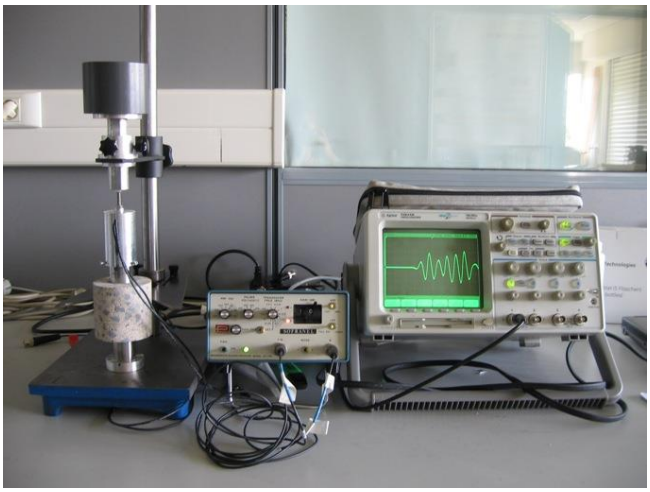

Fig. 1 US transmission device

1.2 Electromagnetic coaxial cylindrical cell

An electromagnetic (EM) cylindrical cell has been designed for the EM characterization of hydraulic and bituminous concrete [38]. This device enables determining the complex dielectric permittivity within the frequency bandwidth of existing Ground Penetrating Radar (GPR) devices,

i.e. from 50 to approx. 1,200 MHz. A coaxial cylindrical transmission line (cell and cables) connected to a vectorial network analyzer has also been designed (Fig. 2). An iterative inversion procedure (Newton-Raphson method) retrieves the material complex permittivity from reflection coefficient measurements [38]. The complex permittivity dispersion curve can then be calculated.

Furthermore, a fitting and extrapolation process dedicated to the dispersion curves obtained by this EM cell is performed by Jonscher's model [39]. The extrapolation steps yield the permittivity at a lower frequency and thus ensure the accuracy of permittivity at both low and high frequencies, corresponding to the devices used for on-site evaluations [39]. The first extracted observable therefore is the real part of the relative permittivity $Eps=\varepsilon_{r\_900MHz}$ (denoted here as permittivity) at 900 MHz, nearly corresponding to the observable obtained on-site with the 1.5 GHz GPR antennas [16] (see Section 3.2). The second one is the real part of the relative permittivity ε_{r_33MHz} at 33 MHz, which roughly corresponds to the observable obtained on site with capacitive probes (yet the corresponding results are not shown herein). For information, the saturated concrete variation range of the permittivity at 900 MHz lies between roughly 6 and 14 [37].

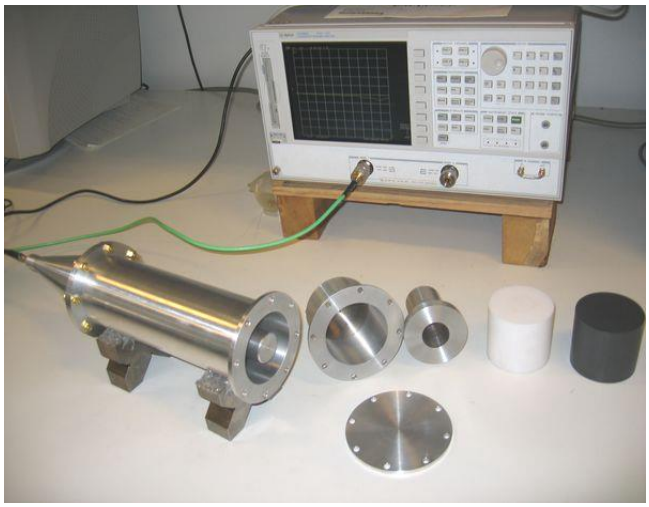

Fig. 2 EM coaxial cylindrical cell

1.3 Electrical multi-electrode cell

An electrical resistivity cell has been designed to measure the resistivity of cylindrical concrete samples [40]. Alternating current is injected on both planar surfaces, and five annular electrodes serve to measure the potential difference between two electrodes corresponding to the

sample resistivity at different heights (Fig. 3). A determination is made of either the local resistivity at various positions or the overall average resistivity of the concrete sample.

The mean value (denoted Re) constitutes the observable similar to the concrete resistivity measured on-site by means of the 10-cm spaced quadrupole used on-site [41]. The saturated concrete variation range of resistivity is about 30-150 Ω.m [37]

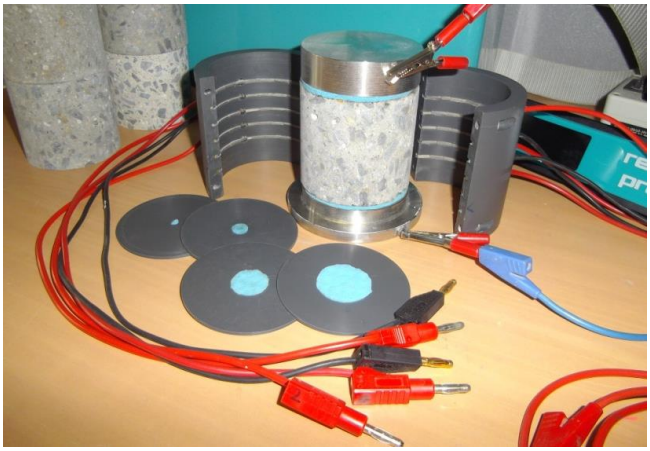

Fig. 3 Resistivity cell

2 CALIBRATION PROTOCOL

The proposed calibration methodology is based on laboratory tests performed on cores extracted from the surveyed structure for the purpose of building representative conversion models (i.e. calibration curves) to transform ND results into durability indicators. An initial ND test, called "pre-auscultation", using rapid on-site ND techniques is required to optimize the localization of future cores. Rapid on-site US techniques, which include impact echo [42, 43, 12], are particularly effective in both evaluating mechanical properties and selecting the coring zones on which the minimum and maximum mechanical characteristics are found. More specifically, the greater the difference between mechanical characteristics, the more accurate is the slope evaluation of linear regression calibration models. The third zone can subsequently be chosen with intermediate properties. The cores are extracted by a coring machine and then carefully wrapped in sealed plastic bags. The laboratory experimental program is summarized in Figure 4 and presented below:

- Phase 0: In the laboratory, the initial mass is measured so as to estimate the initial degree of saturation.
- Phase 1: The samples are saturated with water under vacuum [44], weighed in both air and water, and then tested according to the 3 ND calibration methods.
- Phase 2: The samples are dried in a climatic chamber under controlled conditions (around RH = 80% and T ≈ 65°C) for several weeks until constant mass is achieved. They are then weighed and tested using the 3 ND calibration methods.
- Phase 3: The samples are dried in a climatic chamber under different controlled conditions (around RH = 50% and T ≈ 65°C) for several weeks until constant mass. Likewise, they are then weighed and tested using the 3 ND calibration methods.
- Phase 4: The samples are dried in an oven at T=105°C for several weeks until constant mass in order to obtain the dry mass and determine bulk porosity of the sample [44].

The aim of Phases 2 and 3 is to reach a degree of saturation near S=75% and S=50%; however, since the desorption isotherm linking relative humidity RH and S for a specific concrete mix is unavailable, only a rough approximation of RH is possible. The chosen degrees of saturation are high (above 50%) for two reasons: 1) they better correspond to France's climate and internal concrete conditions; and 2) the relationship between ultrasonic velocity and degree of saturation is no longer a bijection at low degrees of saturation (under ≈30%), as shown and explained by [43,11].

For improved calibration curve accuracy, higher degrees of saturation (i.e. by repeating Phases 2 and 3 multiple times) may be studied, yet the objective entails an operational protocol minimizing the number of testing phases, as well as the number of cores.

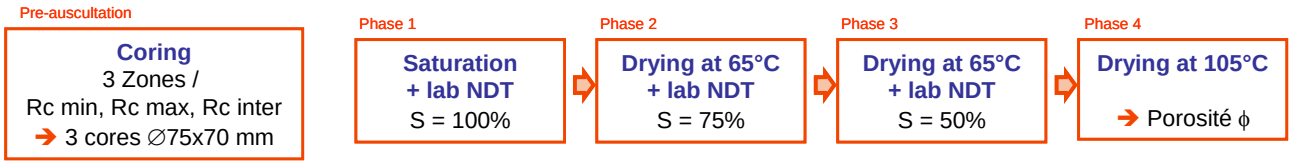

Fig. 4 Calibration protocol flowchart

3 APPLICATION ON A TEST SITE: PILES OF A HIGHWAY BRIDGE IN MARLY

The protocol developed during research project C2D2-ACDC was tested at two sites [31]:

- on three piles of a highway bridge located in northern France (Marly), and
- on three walls of leak-proof tanks at a power plant located near the shore (Le Havre).

The results processed in this paper solely stem from the experimental campaign conducted on the Marly highway bridge.

3.1 Presentation of the structure and localization of ND testing

The tested structure, called the Marly Bridge, is a highway bridge (Fig. 5) set in northern France within a suburb of Valenciennes [31]. This structure, built in 1977-78, is composed of three parallel bridges oriented east-west. Among the 16 piles, three (denoted herein A, B and C) have been chosen based on their exposure to climatic conditions. Pile A is situated under the central bridge, hence under rather protected conditions, whereas Piles B and C are the southern outer piles (B: southeast, and C: southwest), i.e. under conditions more heavily exposed to the wind, sun and rain. The piles are 6 m high and 0.5 m thick; their width increases from 1.8 m to 3 m at the top. The mesh dimension is approximately 0.2 x 0.27 m.

a  b 

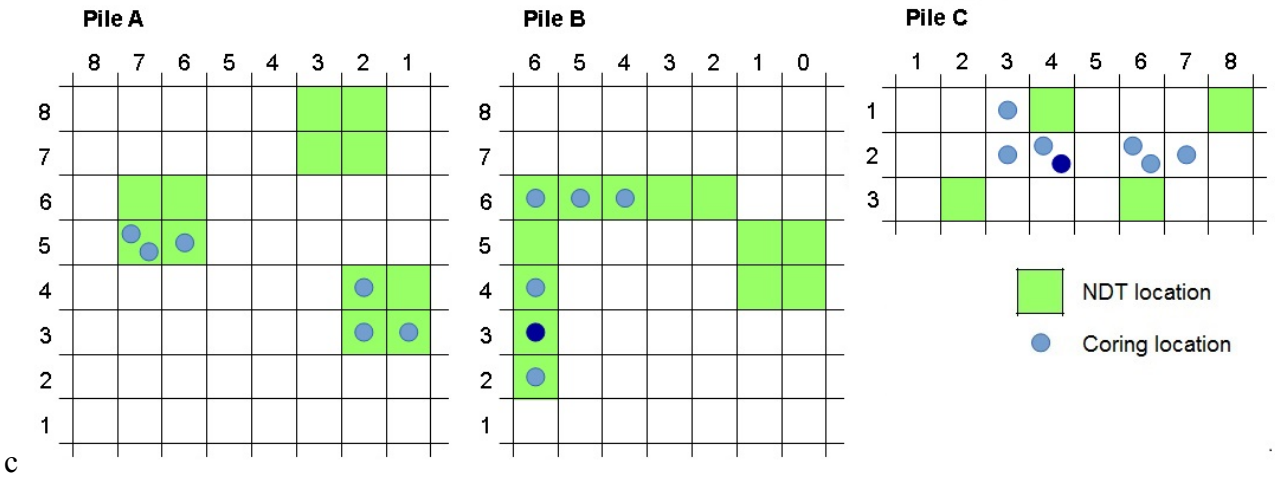

c

Fig 5 Marly Bridge - a) Overview - b) Close-up of the B-pile – c) Measurement points and coring location on the 3 piles

3.2 *In situ* ND measurement methods

Following a rapid initial ND test and data analysis (known as pre-auscultation, as detailed in [31] and recommendations [4]), three zones per pile were identified for possessing the requisite minimum, maximum and intermediate mechanical strength. Each zone is made up of four reinforcement grid meshes. At the center of each mesh, ND parameters were measured using many on-site ND methods [31]. Only three distinct on-site ND methods have been examined in this paper, namely: ultrasonic waves in transmission, GPR, and resistivity measurement techniques. The ND measurement points in the three zones per pile and the coring location are indicated in Fig. 5-c.

The first method consists of measuring the velocity of the ultrasonic pressure (or longitudinal) wave (i.e. P-wave velocity, *Vp*, in m/s) with two piezoelectric US transducers positioned on each pile face, at a distance of 0.5 m [11]. The central frequency of the transmitted signal, which equals 250 kHz, corresponds precisely to that of the US calibration method implemented on cores in the laboratory. Note that scotch tape was used to prevent the contact gel from polluting the studied concrete.

The second method involves two GPR antennas, with a 1.5 GHz nominal central frequency yet transmitting closer to 0.9 GHz for the direct wave on concrete [16], which explains why cores are characterized around this frequency with the EM coaxial cell for in-laboratory calibration. The transmitter and receiver are gradually taken away from one another and the measured signals, from

the direct wave in the material, are analyzed to calculate EM permittivity $Eps=\varepsilon_{r\_900MHz}$. The order of magnitude of the EM wave penetration depth in the concrete is estimated at approx. 10 cm.

The third method studied here is a quadrupole measuring concrete resistivity, as developed in [41]. Two electrodes inject electrical current at roughly 110 Hz and 0.5 mA and the two other electrodes measure the potential difference. Taking the geometry into account, the resistivity *Re* is calculated in taking geometry into account. The electrode role changes, hence the result corresponds to the mean value within the investigated volume. The resistivity measured with the 10-cm spaced quadrupole is preferable to that measured with the 5-cm spaced quadrupole since the investigated volume is deeper, meaning less influenced by skin effects. The resistivity thus better corresponds to sawn cores used in the calibration protocol.

To obtain the mean value and the standard deviation, each ND measurement is repeated minimum 4 times per mesh, per face of each pile. For the study presented herein, it represents 28 mean values (28 meshes visible in Fig. 5-c) for the three ND techniques, thus more than 672 measurement results have been taken into account. This correspond to 28 meshes X 2 faces X 3 techniques X 4 measurements (minimum). Moreover the repeatability standard deviation was determined in the same place, in only one mesh, by determining the mean value of each technique 10 times (10 X 3 techniques X 4 measurements = 120 additional data).

3.3 Coring

After ND testing, 19 cores were removed in the meshes where NDT had been performed (see Fig. 5-c); they were then sawn to obtain cylindrical samples with the right dimensions, in recognizing that the dimensions required for ND calibration are ∅75 x 70 mm, while those for compressive strength and Young's modulus are ∅75 x 150 mm. As regards the samples used to determine porosity ϕ and degree of saturation S for validation purposes, these dimensions are roughly ∅75 x 60 mm.

The ND laboratory calibration protocol described herein was applied on a total of 15 samples, broken down as follows: 3 from Pile C, 3 from Pile B, 5 from Pile A (all of which were extracted from the pile core, i.e. safe concrete), plus 4 additional samples from Pile A extracted at the surface (including the skin and cover concrete submitted to degradation).

Moreover, 17 samples were characterized by means of standardized destructive tests in order to determine the compressive strength R_c [45] and static Young's modulus E_{stat} [46]. For validation, the durability indicators were derived according to the same standardized protocol [44] as for calibration yet in a different laboratory on different samples. ϕ and S were thus determined on 6 core samples (i.e. 3 from Pile C, 2 from Pile B, and 1 from Pile A) and 6 surface samples. The number of cores used in this study is very high given the goal of procedural optimization. The repartition of the core pieces for ND calibration protocol and reference destructive testing campaign is given in Table 1. Thus, it represents 88 destructive testing results (reference and calibration) plus 195 means values for NDE for calibration (around 870 measurements).

Let's also note that all measurement results obtained on cores cannot be considered as true durability indicator values but instead are to be considered as references.

Table 1 Sample repartition for ND calibration campaign and reference destructive testing

Reference destructive testing campaign					
	Samples			Total number of tests	
Pile	***Rc* and E_{stat}**	**ϕ and S_{ini}**		***Rc* and E_{stat}**	**ϕ and S_{ini}**
A	13C, 23C, 24C, 65C, 75aC, 75bC	23C		6	1
B	62C, 64C, 46C, 56C, 66C	62C, 64C, 46C		5	3
		62S, 64S, 46S			3
C	31C, 32C, 42C, 62aC, 62bC, 72C	31C, 32C, 72C		6	3
		31S, 72S			2
ND calibration protocol					
	Samples	Total number of mean values			
Pile	∅75x70 mm	**US cell** S_{ini} and $S \in$ {100, 75, 50%}	**EM cell** S_{ini} and $S \in$ {100, 75, 50, 5%}	**Resistivity cell** S_{ini} and $S \in$ {100, 75, 50%}	**ϕ and S_i**

A	13C, 23C, 24C, 65C, 75bC	20	25	20	5
	13S, 24S, 65S, 75bS	16	20	16	4
B	62C, 64C, 46C	12	15	12	3
C	42C, 62aC, 62bC	12	15	12	3

4 RESULTS AND DISCUSSION

4.1 Calibration curves

The in-laboratory ND (ND-lab) protocol yields several distinct calibration curves corresponding to the conversion models for converting observables into indicators, including the following:

- US P-wave velocity vs. porosity (Fig. 6),
- US P-wave velocity vs. degree of saturation (Fig. 7),
- EM permittivity at 900 MHz vs. degree of saturation (Fig. 8),
- electrical resistivity vs. degree of saturation (Fig. 9),

for the 3 Marly Bridge piles (Pile A in black, Pile B in blue, and Pile C in red).

During a former research project entitled ANR-SENSO [35, 11, 12], certain relationships between observables and indicators were determined in the laboratory. We have opted to compare the calibration curves obtained for Marly Bridge with the relationships obtained in the laboratory on slabs (8 per concrete) under homogeneous conditions, in using the same on-site ND techniques as those used to assess the Marly Bridge pile. The ANR-SENSO results are presented in green in Figures 6 through 9 for two concretes, G3a and G7, whose water-to-cement ratio *W/C* and porosity are similar to those of the Marly Bridge (see Table 2). In Figure 6, results from the ANR-SENSO project correspond to the mean porosity values measured for each of the 6 concrete mixes designed with the same aggregates, with just the *W/C* changing.

Table 2 Concrete mix designs and properties under saturated conditions (sat) for concretes G3a and G7 from the ANR-SENSO project [35] and the Marly Bridge pile concrete

		G3a	G7	Bridge piles
Water-to-cement ratio	*W/C*(-)	0.57	0.68	/
Compressive strength	Rc_{sat} (MPa)	40.5±1.5	38.3±3.0	50.1±5.9
Static Young's modulus	E_{sat} (GPa)	27.9±0.4	27.4±2.8	32.0±2.7
Mean density of the slab/core	ρ_{sat} (kg/m^3)	2447±7	2455±12	2368±27
Bulk porosity	ϕ (%)	16.0±0.7	15.9±0.8	15.7±0.7

One of the main conclusions drawn from the ANR-SENSO project [35] is that US velocity *Vp* is linearly correlated with porosity. This finding seems to be confirmed for the Marly Bridge cores using the ND-lab technique, with a similar slope (Fig. 6), even though these results are highly dispersed. It is more difficult to obtain very different porosities for the same concrete mix on a real structure (which is why minimum and maximum zones were chosen, thus producing a wide range of concrete properties) than in the laboratory on 8 mixes with different water-to-cement ratios (ranging from 0.3 to 0.9). Moreover, the absolute error in porosity determination [5] on 3 cores is about 0.5%-1%, which is not far outside the Marly core porosity variation range (i.e. from 14.1% to 16.3%). Another interesting result is that the surface samples show the same slope (dotted black line and cyan squares) as the others.

These results also confirm (Fig. 7) that the P-wave velocity *Vp* is linearly correlated with the degree of saturation, in the range $45\% \leq S \leq 100\%$, with a similar slope.

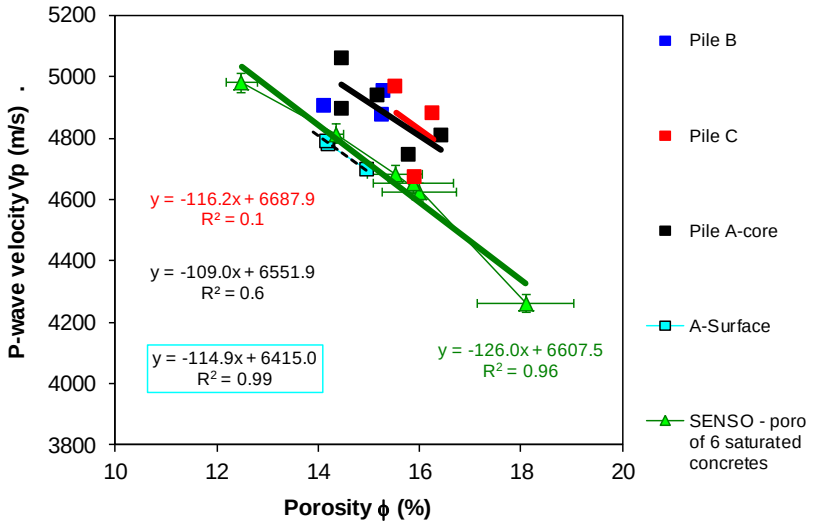

Fig. 6 P-wave velocity vs. porosity for Marly cores and ANR-SENSO slabs

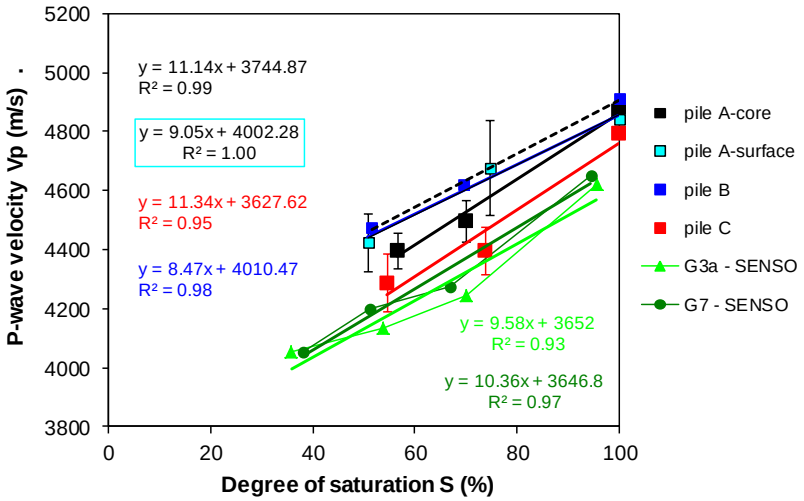

Fig. 7 P-wave velocity vs. degree of saturation for Marly cores and ANR-SENSO slabs

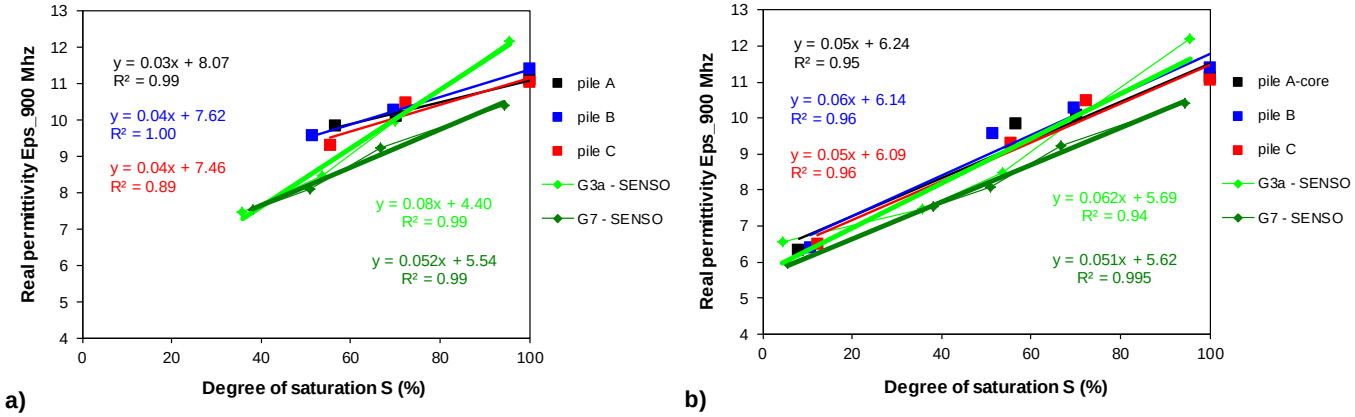

Fig. 8 Permittivity at 900 MHz vs. degree of saturation for Marly cores and ANR-SENSO slabs - a) in the range 40% ≤ S ≤ 100% - b) in the range 0% ≤ S ≤ 100%

As regards EM permittivity, the results obtained on Marly Bridge cores with the ND-lab technique (EM cell) are comparable to those obtained on ANR-SENSO slabs using on-site techniques. Since uncertainty was greater than expected (Fig. 8a), an intermediate phase was added: before drying at T=105°C, which destroys part of the hydrates [47], these samples were dried at T=65°C in an oven until constant mass and then ND-tested. This protocol change allows performing ND tests at much lower water content and improves linear regression accuracy, as seen in Figure 8b.

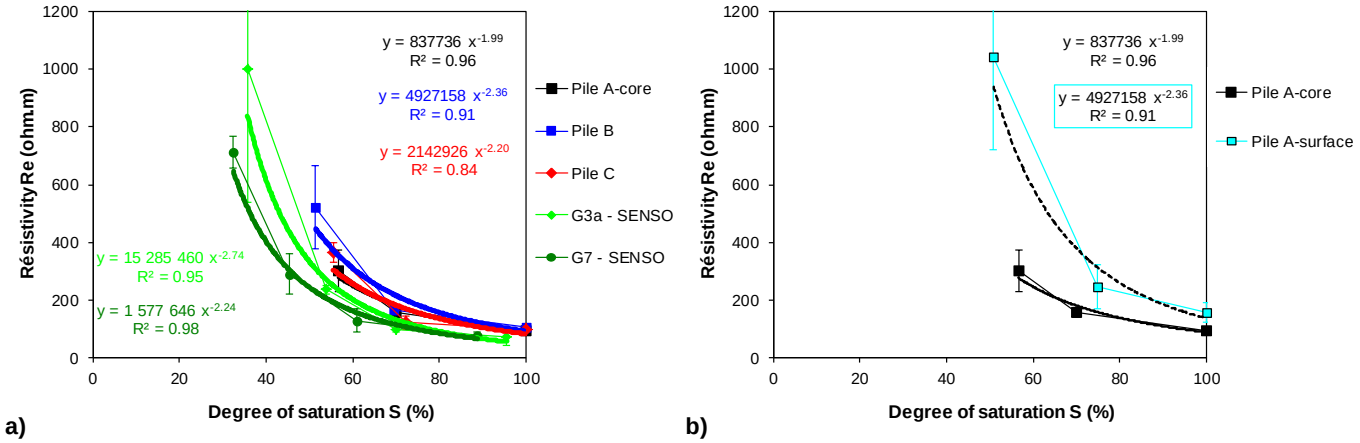

Fig. 9 Resistivity vs. degree of saturation for Marly cores and ANR-SENSO slabs - a) cores from the pile core - b) Pile A: cores from the core and the surface

For electrical resistivity, the results obtained on Marly Bridge cores with the ND-lab technique (resistivity cell) are also comparable to those derived on SENSO slabs using the on-site technique (Fig. 9). Nevertheless, the resistivity measurement is highly sensitive to chemical changes caused by a different hydration of the skin or to degradation-including carbonation. The resistivity cell developed at IFSTTAR [40] is able to determine resistivity gradients from the surface to the core of a structure, as depicted in Figure 10, where the point numbers can be assimilated to apparent depths ranging from 0 to 70 mm and from 75 to 145 mm. When applied on-site therefore, this technique must be very carefully analyzed, depending on the investigation depth of the on-site technique employed. In the following section, in order to evaluate durability indicators using on-site ND measurements with a 10-cm quadrupole on Pile A, calibration curves have been obtained for surface cores extracted from 0 to 70 mm.

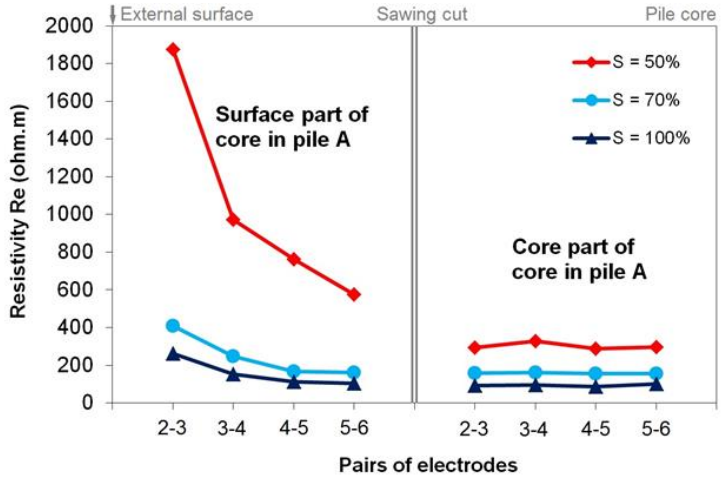

Fig. 10 Resistivity of pairs of annular electrodes for two parts of a core taken in Pile A either the part near the surface (0 mm≤depth≤70 mm) or the part in the pile core (approx. 75 mm≤depth≤145 mm)

4.2 Calibration curve uses when estimating on-site durability indicators

These calibration curves may be used to estimate the durability indicators (porosity and degree of saturation in the present case) thanks to the ND observables determined on Marly Bridge by means of on-site methods. For each ND observable *Yi* among (*Vp*, *Eps*, *Re*), a double linear regression dependent on porosity and degree of saturation can be calculated by relying on ND-lab results, as explained in [12], thus producing an equation such as the following:

$$\mathrm{Ai}.S + \mathrm{Bi}.\phi + \mathrm{Ki} = \mathrm{Yi} \quad (1)$$

Coefficients Ai, Bi, Ci and Ki are all calculated according to the least squares method by solving the following matrix system:

$$[Y] = [B] \times [X] + err \quad (2)$$

with [*Y*] the NDT vector, [*B*] the coefficients matrix, [*X*] the vector of concrete durability indicators, and *err* a small error.

Next, by means of system inversion, the corresponding NDT observables obtained on-site enable assessing the durability indicators. For each tested pile mesh, both durability indicators are estimated by using either 2 observables (*Vp*, *Eps*) or 3 (*Vp*, *Eps*, *Re*) given that resistivity was only measured on Pile A. For each pile, the mean value and standard deviation are then calculated.

Validation of this calibration methodology

First of all, for validation purposes, the estimated and measured durability indicators will be compared. Table 3 lists the values estimated by NDT and those measured with reference standard destructive methods performed on different cores in another laboratory (to ensure independence). We have opted to compare the results in meshes where on-site NDT were performed and cores extracted (same mesh except for Pile C, which was impossible, requiring the immediate neighbor to

be chosen). In Table 3, the estimated and measured indicators are quite similar. The standard deviation is relatively high because of a pre-auscultation process that leads to choosing areas with the greatest differences in terms of mechanical properties and thus most certainly in terms in porosity. Moreover, the uncertainty in the estimated degree of saturation is higher than the measured value, which may be due to either the coring and core conservation conditions or the difference between the pile concrete surface and core. The surface is in fact subjected to precipitations and degradations, which induce gradients and chemical changes while also inducing differences between on-site surface measurements of resistivity and permittivity. In this study, the calibration curves have been determined on core samples for permittivity.

Consequently, this comparison validates the calibration methodology proposed as well as the conversion models obtained in this way.

Table 3 Comparison of estimated durability indicators by using on-site NDT, in addition to conversion models, with reference durability indicators measured on other cores

	On-site localization		Mean estimations ± standard deviation		Ref. measurements on cores	
Pile	NDT	Coring	ϕ (%)	S (%)	ϕ (%)	S (%)
A	1 mesh (Vp ; Eps ; Re)	1 other core in the same mesh	16.6	73.4	15.2	72.3
B	3 meshes (Vp ; Eps)	3 other cores in the same mesh	16.9 ± 3.9	68.2 ± 6.8	16.1 ± 1.2	75.1 ± 1.9
C	3 meshes (Vp ; Eps)	2 other cores in an adjacent mesh	15.4 ± 0.3	78.2 ± 3.4	15.7 ± 0.4	76.1 ± 0.2

Use of 2 or 3 on-site NDT observables

As a second step and in order to decrease uncertainty, 3 observables (Vp ; Eps ; Re) instead of 2 (Vp ; Eps) can be used to estimate the two indicators ϕ and S. Due to available testing results (on-site NDT + cores), this estimation step can only be observed on Pile A for those cores used to build the conversion models, as presented in Table 4, which does not change the estimated porosity. The use of resistivity, highly sensitive to S, enables correcting the estimated degree-of-saturation values: using 3 observables thus increases accuracy.

Table 4 Comparison of estimated and measured durability indicators by using 2 or 3 on-site ND observables

	On-site localization		Mean estimations ± standard deviation		Ref. measurements on cores	
Pile	NDT	Coring	ϕ (%)	S (%)	ϕ (%)	S (%)
A	5 meshes (Vp ; Eps ; Re)	5 cores used for ND calibration	16.3 ± 0.5	73.9 ± 2.3	15.3 ± 0.8	73.1 ± 2.8
A	5 meshes (Vp ; Eps)	5 cores used for ND calibration	16.2 ± 0.4	80.7 ± 1.8	15.3 ± 0.8	73.1 ± 2.8

4.3 Possibility of reducing the number of cores used for calibration

The European standard EN 13791 [48] specifies that for compressive strength assessment from NDT methods (rebound hammer or ultrasonic pulse velocity) at least 9 cores are necessary in each area where a conversion model has to be calibrated. The standard specifies that the 9 cores must be extracted from points on which NDT measurements were performed.

In this study, only 11 cores (5 for Pile A, 3 for Piles B and C) were used for the calibration of all the conversion models. The results show that this number was enough in this case to assess the durability indicators (ϕ and S) with an acceptable prediction error.

Meanwhile, this project has offered the chance and opportunity to make use of a large number of cores on the same bridge. Yet such may not be the case in the future. For this reason, the issue of reducing the number of cores to just 3 (among the 5) cores of Pile A was explored. This investigation corresponds to 10 cases required to build the calibration curves.

First, these 10 cases are applied to the 5 on-site ND measurements in order to estimate the durability indicators and draw comparisons between measured values and calculated residuals (root mean square difference) for the 6 meshes of Pile A. Two cases were easily deleted due to aberrant degree-of-saturation values (above 100% or under 30%). One case was questionable because of high porosity value dispersion, hence higher residuals; nevertheless, the estimated mean porosity was similar to the measured value, as were the calculated degrees of saturation. As for the other 7 cases, the estimated and measured durability indicators were very close to one another, with residuals lying between 0.11 and 0.22 for ϕ, 0.19 and 0.26 for S. By comparison, the residuals equal 0.24 and 0.17 in cases corresponding to Table 3, with calibration curves determined from 5 cores.

Second, the 10 cases are applied to the 3 on-site ND measurements on Pile B and the 3 such measurements on Pile C so as to estimate the durability indicators. Once the 3 doubtful cases were rejected, the estimated values lie very close to the measured values of porosity and degree of saturation. For Pile B, the residuals are respectively between 0.05 and 0.19 for ϕ, 0.11 and 0.26 for S. For Pile C, the residuals are between 0.03 and 0.17 for ϕ, 0.05 and 0.19 for S. By applying the calibration curves determined with cores from the same pile, these results are slightly more dispersed for Pile B (residuals between 0.19 and 0.25) and better for Pile C (between 0.04 and 0.08).

It is possible therefore to reduce the number of cores required to generate the calibration curves, however the risk of an incorrect evaluation is then increased. Moreover, the calibration curves obtained on a given pile may be used to evaluate the durability indicators of other piles provided the same concrete mix design.

CONCLUSION

A laboratory calibration protocol on cores extracted from a surveyed structure was developed and validated on a highway bridge. These cores were extracted from zones identified by means of rapid ND techniques. This protocol served to determine, by ND techniques, the values of ultrasonic P-wave velocity, radar permittivity and resistivity applied on these cores in laboratory. Meanwhile, in implementing standard destructive techniques, the degree of saturation and porosity could be evaluated. The resulting conversion models established in laboratory (or calibration curves) could thus be applied to on-site ND measurements in order to evaluate the on-site durability indicators. These indicators estimated by ND lie very close to the reference indicators measured with standard destructive methods on other cores in another laboratory. The comparisons performed enabled validating a protocol that is applicable to any type of structure. The influence of the actual concrete mix design and material variability can then be taken into account.

This calibration methodology is proposed for the dual purpose of analyzing on-site NDT measurements and obtaining durability indicators, such as porosity and degree of saturation. In a similar manner, compressive strength and water content can be assessed as well.

In order to increase the accuracy of estimated values, two options are proposed. First, as regards mechanical properties and porosity, a pre-auscultation by rapid NDT techniques makes it possible to choose those of zones with the greatest differences in these properties in order to get the largest range of properties variability in the conversion model. Second, a greater number of ND observables than indicators can also decrease the estimation uncertainty.

An analysis of results indicates that this calibration protocol is reliable and useful in correctly evaluating comprehensive mechanical and durability indicators and assessing the concrete conditions of tested structures. Such an analysis however also underscores that further research is needed in order to better account for property gradients in the cover concrete due to skin effects, drying or the penetration of aggressive agents. Reducing the number of cores and the risk of a false evaluation must be more carefully studied.

DECLARATION

The authors declare that they have no conflict of interest.

REFERENCES

[1] Bungey J H, Millard S G (1996) Testing of concrete structures. 3rd ed. Blackie academic & professional, Chapman & Hall, Glasgow, 296 p.

[2] McCann D M, Forde M C (2001) Review of NDT methods in the assessment of concrete and masonry structures, NDT&E International, 34(2): 71–84.

[3] Orcesi A, Frangopol D M (2011) Optimization of bridge maintenance strategies based on structural health monitoring information. Structural Safety, 33(1): 26-41. http://dx.doi.org/10.1016/j.strusafe.2010.05.002

[4] Salin J, Garnier V, Dérobert X, Martini V, Balayssac J-P, Villain G, Fardeau V (2014) Recueil de recommandations - Analyse et Capitalisation pour le Diagnostic des Constructions, Concevoir et Construire pour le Développement Durable. Projet C2D2-ACDC, 74 p.

[5] Baroghel-Bouny V. *et al.* (2007) Concrete design for a given structure service life – Durability management with regard to reinforcement corrosion and alkali-silica reaction – State of the art and guide for the implementation of a predictive performance approach based upon durability indicators. Scientific and technical documents AFGC, (French version 2004), English version 252 p.

[6] Alexander M, Ballim Y, Stanish K (2008) A framework for use of durability indexes in performance-based design and specifications for reinforced concrete structures. Materials and Structures 41: 921–936. http://dx.doi.org/10.1617/s11527-007-9295-0

[7] Bentur A, Diamond S, Berke N S (1997) Steel Corrosion in Concrete – Fundamentals and Civil Engineering Practice, E&FN SPON, London, United Kingdom.

[8] Raharinaivo A, Arliguie G, Chaussadent T, Grimaldi G, Pollet V, Tache G (1998) La corrosion et la protection des aciers dans le béton. Presses de l'école nationale des Ponts et Chaussées, Paris.

[9] Hernández M G, Izquierdo M A G, Ibáñez A, Anaya J J, Ullate L G (2000) Porosity estimation of concrete by ultrasonic NDE. Ultrasonics, 38(1-8): 531-533.

[10] Lafhaj Z, Goueygou M, Djerbi A, Kaczmarek M (2006) Correlation between porosity, permeability and ultrasonic parameters of mortar with variable water / cement ratio and water content. Cement and Concrete Research. 36(4): 625-633. http://dx.doi.org/10.1016/j.cemconres.2005.11.009

[11] Garnier V, Piwakowski B, Abraham O, Villain G, Payan C, Chaix J-F (2013) Acoustical techniques for concrete evaluation: Improvements, comparisons and consistencies. Construction and Building Materials, 43(6): 598–613. http://dx.doi.org/10.1016/j.conbuildmat.2013.01.035

[12] Villain G, Sbartaï Z M, Dérobert X, Garnier V, Balayssac J-P (2012) Durability diagnosis of a concrete structure in a tidal zone by combining NDT methods: laboratory tests and case study. Construction and Building Materials, 37: 893–903. http://dx.doi.org/10.1016/j.conbuildmat.2012.03.014

[13] Ohdaira E, Masuzawa N (2000) Water content and its effect on ultrasound propagation in concrete - the possibility of NDE. Ultrasonics, 38(1-8): 546-552. http://dx.doi.org/10.1016/S0041-624X(99)00158-4

[14] Robert A (1998) Dielectric permittivity of concrete between 50 MHz and 1 GHz and GPR measurements for building materials evaluation. Journal of Applied Geophysics, 40: 89-94,

[15] Soutsos M N, Bungey J H, Millard S G, Shaw M R, Patterson A (2001) Dielectric properties of concrete and their influence on radar testing. NDT&E International, 34(6): 419-425.

[16] Dérobert X, Iaquinta J, Klysz G, Balayssac J P (2008) Use of capacitive and GPR techniques for non-destructive evaluation of cover concrete. NDT&E International, 41: 44-52.

[17] Sbartaï Z M, Laurens S, Rhazi J, Balayssac J P, Arliguie G (2007) Using radar direct wave for concrete condition assessment: Correlation with electrical resistivity. Journal of Applied Geophysics, 62(4): 361-374.

[18] Hugenschmidt J, Loser R (2008) Detection of chlorides and moisture in concrete structures with GPR. Materials and Structures, 41: 785-792.

[19] Lai WL, Kind T, Kruschwitz S, Wöstmann J, Wiggenhauser H (2014) Spectral absorption of spatial and temporal ground penetrating radar signals by water in construction materials. NDT & E International, 67: 55-63.

[20] Kwon SJ, Feng MQ, Park SS (2010) Characterization of electromagnetic properties for durability performance and saturation in hardened cement mortar. NDT & E International, 43(2): 86-95. http://dx.doi.org/10.1016/j.ndteint.2009.09.002

[21] Polder R, Andrade C, Elsener B,Vennesland Ø, Gulikers J, Weidert R, Raupach M (2000) Test methods for on site measurement of resistivity of concrete. Materials and Structures, 33(10): 603-611. http://dx.doi.org/10.1007/BF02480599

[22] van Noort R, Hunger M, Spiesz P (2016) Long-term chloride migration coefficient in slag cement-based concrete and resistivity as an alternative test method. Construction and Building Materials, 115:746-759. http://dx.doi.org/10.1016/j.conbuildmat.2016.04.054

[23] Hallaji M, Seppänen A, Pour-Ghaz M (2015) Electrical resistance tomography to monitor unsaturated moisture flow in cementitious materials. Cement and Concrete Research, 69: 10-18. http://dx.doi.org/10.1016/j.cemconres.2014.11.007

[24] Du Plooy R, Villain G, Palma Lopes S, Ihamouten A, Dérobert X, Thauvin B (2015) Electromagnetic non-destructive evaluation techniques for the monitoring of water and chloride ingress into concrete: a comparative study. Materials and Structures, 48: 369–386, http://dx.doi.org/10.1617/s11527-013-0189-z

[25] Tumidajski, P, Schumacher A, Perron S, Gu P, Beaudoin J (1996) On the relationship between porosity and electrical resistivity in cementitious systems, Cement and Concrete Research, 26(4): 539-544.

[26] Maierhofer C, Zacher G, Kohl C, Wöstmann J (2008) Evaluation of radar and complementary echo methods for NDT of concrete elements. Journal of Nondestructive Evaluation, 27:47–57.

[27] Breysse D, Klysz G, Dérobert X, Sirieix C, Lataste J-F (2008) How to combine several non-destructive techniques for a better assessment of concrete structures. Cement and Concrete Research, 38(6): 783-793. http://dx.doi.org/10.1016/j.cemconres.2008.01.016

[28] Sbartaï Z M, Breysse D, Larget M, Balayssac J-P (2012) Combining NDT techniques for improving concrete properties evaluation. Cement and Concrete Composites, 34(6): 725-733. http://dx.doi.org/10.1016/j.cemconcomp.2012.03.005

[29] Alani A. M, Aboutalebi M, Kilic G (2014) Integrated health assessment strategy using NDT for reinforced concrete bridges. NDT & E International, 61: 80-94. https://doi.org/10.1016/j.ndteint.2013.10.001

[30] Rivard P, Saint-Pierre F (2009) Assessing alkali-silica reaction damage to concrete with non-destructive methods: From the lab to the field. Construction and Building Materials, 23:902-909. https://doi.org/10.1016/j.conbuildmat.2008.04.01

[31] Garnier V, Martini D, Salin J, Fardeau V, Sbartaï Z M, Breysse D, Piwakowski B, Villain G, Abraham O, Balayssac J-P (2014) Non Destructive Testing of Concrete: Transfer from Laboratory to On-site Measurement. *7th European Workshop on Structural Health Monitoring*, Nantes, France, 8-11 July 2014, 8p. https://hal.inria.fr/hal-01021045/document

[32] Aggelis D G, Shiotani T (2008) Surface wave dispersion in cement-based media: Inclusion size effect, NDT & E International, 41(5), 2008: 319-325, https://doi.org/10.1016/j.ndteint.2008.01.010

[33] Dérobert X, Villain G (2017) Development of a multi-linear quadratic experimental design for the EM characterization of concretes in the radar frequency-band, Construction and Building Materials, 136: 237–245. http://dx.doi.org/10.1016/j.conbuildmat.2016.12.061

[34] Gomez-Cardenas C., Outils d'aide à l'optimisation des campagnes d'essais non destructifs sur ouvrages en béton armé, PhD report, Université de Toulouse, 4 December 2015, 174p.

[35] Balayssac J-P, Laurens S, Arliguie G, Breysse D, Garnier V, Dérobert X, Piwakowski B (2012) Description of the general outlines of the French project SENSO - Quality assessment and limits of different NDT methods. Construction and Building Materials, 35: 131–138. http://dx.doi.org/10.1016/j.conbuildmat.2012.03.003

[36] Benmeddour F, Villain G, Abraham O, Choinska M (2012) Development of an ultrasonic experimental device to characterise concrete for structural repair. Construction and Building Materials, 37(12): 934–942. http://dx.doi.org/10.1016/j.conbuildmat.2012.09.038

[37] Balayssac J-P and Garnier V (2017) Non-destructive Testing and Evaluation of Civil Engineering Structures, Eds by Balayssac and Garnier, ISTE Press – Elsevier, Nov. 2017, 376p. ISBN: 9780081023051

[38] Adous M, Queffelec P, Laguerre L (2006) Coaxial/cylindrical transition line for broadband permittivity measurement of civil engineering materials. Meas. Sci. Technol. 17: 2241–2246.

[39] Villain G, Ihamouten A, Dérobert X (2017) Determination of concrete water content by coupling electromagnetic methods: Coaxial/cylindrical transition line with capacitive probes. NDT & E International, 88: 59-70. http://dx.doi.org/10.1016/j.ndteint.2017.02.004

[40] Du Plooy R, Palma Lopes S, Villain G, Dérobert X (2013) Development of a multi-ring resistivity cell and multi-electrode resistivity probe for investigation of cover concrete condition. NDT and E International, 54: 27–36. http://dx.doi.org/10.1016/j.ndteint.2012.11.007

[41] Lataste J-F, Sirieix C, Breysse D, Frappa M (2003) Electrical resistivity measurement applied to cracking assessment on reinforced concrete structures in civil engineering. NDT & E International, 36(6): 383-394. http://dx.doi.org/10.1016/S0963-8695(03)00013-6

[42] Sansalone M J, Streett W B (1997) Impact echo: non-destructive evaluation of concrete and masonry. Bullbrier Press, 339p.

[43] Villain G, Le Marrec L, Rakotomanana L (2011) Determination of the bulk elastic moduli of various concretes by resonance frequency analysis of slabs submitted to impact echo. European Journal of Environmental and Civil Engineering, 15(4): 601-617. http://dx.doi.org/10.1080/19648189.2011.9693350

[44] AFPC-AFREM (1997) Compte-rendu des journées techniques de l'AFPC-AFREM, Durabilité des Bétons, Méthodes recommandées pour la mesure des grandeurs associées à la durabilité. 11 et 12 décembre 1997, Toulouse, 284p.

[45] EN 12390-3: 2009 Testing hardened concrete. Compressive strength of test specimens, 22p.

[46] EN 13412: 2006 Products and systems for the protection and repair of concrete structures. Test methods. Determination of modulus of elasticity in compression, 12p.

[47] Zhou Q, Glasser F P (2001) Thermal stability and decomposition mechanisms of ettringite at <120°C, Cement and Concrete Research, 31(9): 1333-1339. https://doi.org/10.1016/S0008-8846(01)00558-0

[48] EN 13791: 2007 Assessment of in-situ compressive strength in structures and precast concrete components, 28p.